Rock and Soil Mechanics

Volume 43 | Issue 11 Article 8

1-15-2023

A rapid determination method of hydraulic conductivity in full suction range

A-qiang LIU

Xu LI
xuli@bjtu.edu.cn

Yan LIU

Zhi-yuan ZHANG

Custom Citation
LIU A-qiang, LI Xu, LIU Yan, ZHANG Zhi-yuan. A rapid determination method of hydraulic conductivity in full suction range[J]. Rock and Soil Mechanics, 2022, 43(11): 3209-3219.

Rock and Soil Mechanics 2022 43(11): 3209–3219 ISSN 1000–7598
https: //doi.org/10.16285/j.rsm.2022.5004 rocksoilmech.researchcommons.org/journal

A rapid determination method of hydraulic conductivity in full suction range

LIU A-qiang, LI Xu, LIU Yan, ZHANG Zhi-yuan

Key Laboratory of Urban Underground Engineering of Ministry of Education, Beijing Jiaotong University, Beijing 100044, China

Abstract: The hydraulic conductivity function of unsaturated soil spans several orders of magnitude. Traditional measurement methods often take several months, and it is difficult to measure the hydraulic conductivity in the full suction range. In order to realize the rapid measurement of hydraulic conductivity in the full suction range, the wetting front advancing method is combined with the instantaneous profile method (here referred to as the combined determination method) in this study. A self-developed soil column infiltration device was used to measure the hydraulic conductivity of Qinghai silty clay in the full suction range under different dry densities. The test results show that in the combined determination method, the wetting front advancing method is suitable for the measurement of hydraulic conductivity in the high suction range ($\psi > 25$ kPa), while the instantaneous profile method is suitable for measuring the hydraulic conductivity in the low suction range ($\psi \leqslant 25$ kPa). The hydraulic conductivity determined by the two methods in the overlapped suction range is basically consistent. The combined determination method can reduce the measurement time of hydraulic conductivity in the full suction range by about one week with good accuracy. In addition, the error sources of the two measurement methods are also analyzed and discussed in this work. The results show that the combined determination method can realize the rapid measurement of hydraulic conductivity in the full suction range, which is expected to make the measurement of the hydraulic conductivity of unsaturated soil become a routine test in soil mechanics.

Keywords: full suction range; rapid determination; hydraulic conductivity; wetting front advancing method; instantaneous profile method

1 Introduction

The soils in nature and involved in practical engineering are mostly in the unsaturated state. Unlike saturated soil, the hydraulic conductivity of unsaturated soil constantly changes with soil suction or water content, and its variation range s several orders of magnitude. The soil hydraulic conductivity function (SHCF) is an essential parameter in the seepage flow analysis of unsaturated soil. The accuracy and timeliness of the measurement of SHCF directly determine the solving precision of the unsaturated seepage problem.

At present, the commonly used testing methods for measuring the hydraulic conductivity of unsaturated soil can be classified into indirect method and direct method. The indirect method is used to evaluate SHCF based on soil-water characteristic curve (SWCC)[1–4], pore size distribution curve[5–9], and grading curve[10–11]. However, the predicted results may not be in satisfactory agreement with the measured results[12–13]. The direct method measures SHCF through laboratory tests, which can be classified into steady state method and unsteady state method. Based on the steady state method, Huang et al.[14] and Samingan et al.[15] determined the hydraulic conductivity of unsaturated soil using a self-developed flexible wall permeameter. The unsteady state method is further classified into instantaneous profile method (IPM) and wetting front advancing method (WFAM). IPM was pioneered by Richards et al.[16], later being widely used. Based on IPM, Cui et al.[17], Wang et al.[18] , Ye et al.[19–20], Niu et al.[21], and Liu et al.[22] measured the temperature and relative humidity during the test with the temperature and humidity sensors and studied the permeability characteristics of densely compacted Gaomiaozi bentonite under the condition of partial free expansion at constant volume. However, these tests took a long time (from several months to a year). Hu et al.[23–24] used IPM to measure the hydraulic conductivity of unsaturated loess. However, due to the excessive infiltration rate and large sensor spacing in the test, the hydraulic conductivity obtained from the test had a large error. WFAM was pioneered by Li et al.[25]. This method does not need to strictly control the infiltration rate, but only needs to measure the wetting front advancing rate and the monitoring data of water content and suction of a section to determine SHCF. Compared to the steady state method and IPM, WFAM can reduce the measurement duration of hydraulic conductivity from several months to several days, thus it has broad application prospects. Based on WFAM, Miao et al.[26] conducted the capillary water rising tests on the unsaturated clay-containing sand with different initial water contents, and the results showed that the hydraulic conductivity of unsaturated soil can be quickly determined by the variations of wetting front advancing rate, water content and suction. Li et al.[27] and Liu et al.[28] verified the measurement accuracy and application

Received: 5 January 2021 Revised: 13 July 2022
This work was supported by the National Natural Science Foundation of China (51979002) and Beijing Natural Science Foundation (8192034).
First author: LIU A-qiang, male, born in 1996, Master student, focusing on unsaturated soil seepage research. E-mail: 19125866@bjtu.edu.cn
Corresponding author: LI Xu, male, born in 1980, PhD, Professor, mainly engaged in research on special soils mechanics, computational rock and soil mechanics, machine learning in geotechnical engineering applications. E-mail: xuli@bjtu.edu.cn

range of WFAM by means of numerical simulation. It is found that WFAM can measure the hydraulic conductivity in a wide suction range, and the initial water content, sensor spacing and wetting front threshold have no apparent effect on the measurement accuracy of WFAM. In addition, Qin et al.[29], Liu et al.[30] and Cai et al.[31] also adopted WFAM to explore the hydraulic conductivity of unsaturated soil.

Although the steady state method, IPM and WFAM can obtain the function of hydraulic conductivity, these three test methods have their own limitations. The steady state method has a narrow measuring range and requires strict control of inlet flow to achieve a stable state, which is often time-consuming. Similarly, the test duration of IPM generally lasts several months, and the hydraulic conductivity measured in the high suction range often has a large error[24]. Compared to the other two methods, WFAM can greatly reduce the test duration. However, when the soil transitions from unsaturated state to saturated state, i.e. after the wetting front disappears, this method can no longer play an effective role. Therefore, WFAM is also unable to measure the hydraulic conductivity in the full suction range. To sum up, there is still a lack of an effective method to measure SHCF in the full suction range within a relatively short period of time (such as one week), thus it is still a great challenge to rapidly measure SHCF in the full suction range.

Li et al.[32] used numerical tests to verify that the combined determination method could quickly measure the hydraulic conductivity in the full suction range. In order to verify the effectiveness of the combined determination method in laboratory tests, this study measured the SHCF of Qinghai silty clay under different dry densities using a self-developed soil column infiltration device. This method can realize the rapid determination of soil hydraulic conductivity in the full suction range in the same set of equipment and can quantitatively analyze the test error and application range of WFAM and IPM. Finally, a set of standardized testing procedures is established.

2 Testing principles

WFAM proposed by Li et al.[25] was adopted in this study. Based on the linear assumption in the time domain, this method allows time to approach a small increment. It is assumed that the contour of water content in the wetting area advances steadily in the process of infiltration. During the test, the variations of wetting front, water content and matric suction with time were continuously recorded, and then the hydraulic conductivity was calculated according to the following formula:

$$k = \frac{(\theta_2 + \theta_1 - 2\theta_0)}{2(\psi_1 - \psi_2 + \gamma_w v \cdot \Delta t)} \gamma_w v^2 \cdot \Delta t \quad (1)$$

where k is the average hydraulic conductivity at the times t_1 and t_2, and the corresponding suction is 0.5 ($\psi_1 + \psi_2$); ψ_1 and ψ_2 are the matric suctions of the monitoring section at the times t_1 and t_2; θ_0 is the initial volume water content; θ_1 and θ_2 are the volume water contents of the monitoring section at the times t_1 and t_2; Δt is the time difference, i.e. ($t_2 - t_1$); γ_w is the unit weight of water; and v is the wetting front advancing rate.

IPM is based on spatial linear assumptions (i.e. linear assumptions at adjacent monitoring sections). A series of moisture and suction sensors was installed along the soil column, and periodical monitoring was performed to obtain the distributions of water content and suction along the whole soil column. Then, the hydraulic conductivity was calculated according to the following formula:

$$k = \frac{q\gamma_w L}{(\psi_{s1} - \psi_{s2} + \gamma_w L) S \cdot \Delta t} \quad (2)$$

where q is the flow through a monitoring section within a time interval Δt; L is the distance between two adjacent monitoring sections; ψ_{s1} and ψ_{s2} are the suctions of two adjacent monitoring sections; and S is the cross-sectional area of the soil column.

The detailed introduction and theoretical derivation of WFAM and IPM can be found in Li et al.[25] and Daniel et al.[33].

3 Testing methods

3.1 Testing program

The soil used in the test is silty clay sampled from the vicinity of Xiangpi Mountain National Highway in Gonghe County, Qinghai Province, China. According to the *Standard for Geotechnical Testing Method* (GB/T50123–2019)[34], the basic physical properties of this soil were measured, as shown in Table 1. The particle grading curves were measured using sieving and hydrometer method, as shown in Fig. 1. Through calculation, the coefficient of uniformity is $C_u = 9.38$ (> 5), and the coefficient of curvature is $C_c = 2.38$ (between 1 and 3), thus this soil is well graded.

Table 1 Basic physical properties of Qinghai silty clay

Soil type	Liquid limit W_L /%	Plastic limit W_P /%	Maximum dry density /(g • cm^{-3})	Optimum water content /%	Specific gravity G_S
Qinghai silty clay	27.2	15.1	1.75	15.5	2.7

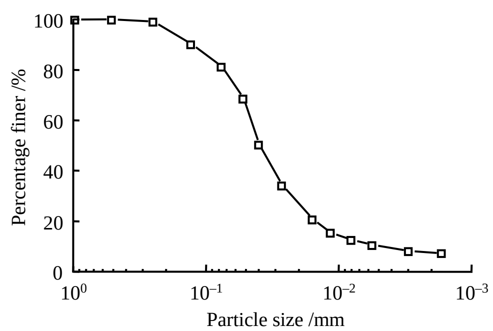

Fig. 1 Gradation curve of Qinghai silty clay

In order to explore the feasibility of using combined determination method to measure the hydraulic conductivity of soil in the full suction range, a series of soil column infiltration test was carried out. The naturally air-dried Qinghai silty clay with initial water content of 0.85% was used in the test to obtain the SHCF in the full suction range. The samples were prepared by compaction in layers. There were 20 layers in total and each layer was compacted with 2 cm. Three tests were carried out with dry densities of 1.58, 1.49 and 1.40 g/cm^3, respectively.

In order to meet the requirements of the data analysis of soil column infiltration test, the SWCC rapid determination method proposed by Li et al.[35] was used first to measure the SWCC of soil samples with different dry densities. The test results are shown in Fig. 2, and the fitting parameters of the corresponding VG model[36] are listed in Table 2.

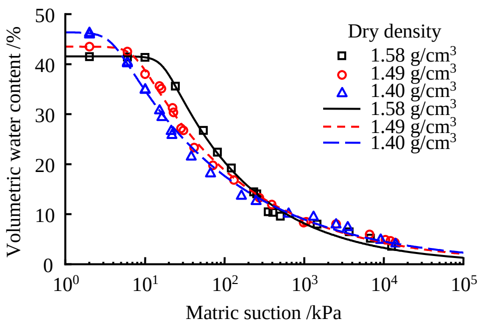

Fig. 2 SWCCs of Qinghai silty clay

Table 2 Fitting parameters of VG model for SWCC of Qinghai silty clay

Dry density /(g • cm^{-3})	a /kPa^{-1}	Fitting parameters n	m
1.58	0.059	5.332	0.075
1.49	0.136	4.549	0.071
1.40	0.264	4.335	0.068

Note: a is the parameter related to the air entry value; n is the parameter related to the slope of SWCC; m is the parameter related to the overall symmetry of SWCC.

3.2 Testing apparatus

In this study, a self-developed soil column infiltration equipment was used to conduct the combined determination tests of soil hydraulic conductivity in the full suction range. This testing apparatus mainly includes soil column mold, data acquisition system and water supply (drainage) system, as shown in Fig. 3.

The soil column mold is a cylinder made of highly transparent acrylic material, with an inner diameter of 100 mm, a wall thickness of 5 mm and a height of 400 mm. In order to facilitate compaction, the total length of the soil column was processed to 450 mm, and a perforated plate with a thickness of 10 mm was arranged on the bottom plate of the soil column. In the test, three SM926 moister sensors and three TEROS31 suction sensors (Fig. 3(a)) were installed to monitor the variations of water content and suction over time. Only the probes of the moisture sensor were inserted into the soil column. The diameter of the probe is 4 mm and the length is 50 mm, with a four-claw structure. The suction sensor measured the suction of soil through a ceramic head that has a diameter of 5 mm and a length of 8 mm. The moisture sensor and suction sensor are distributed symmetrically with equal spacing, as shown in Fig. 3(b). The water content, suction and mass of water inflow and outflow in the test can be recorded through the data acquisition system. The data of water content and suction were collected by CR1000 data acquisition instrument, and the acquisition interval was 10 s. The mass of water inflow and outflow was collected by digital acquisition electronic balance with accuracy of 0.1 g (measuring range of 15 kg) and 0.01g (measuring range of 2 kg).

(a) Moisture sensor (left) and suction sensor (right)

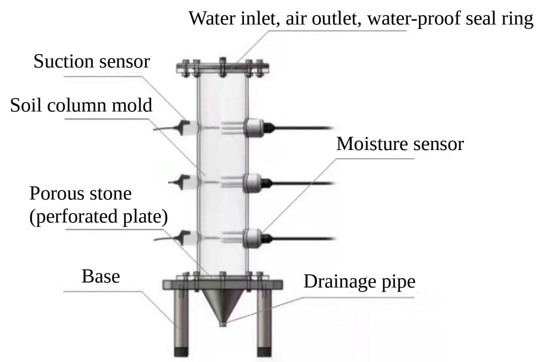

(b) Soil column mold

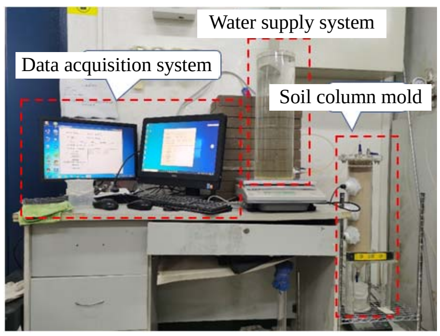

(c) Testing apparatus

Fig. 3 Test device

The water supply system adopted Mariotte's bottles[37] with an inner diameter of 150 mm and a height of 500 mm, which can provide the infiltration conditions of constant water head for the soil column. The water in the Mariotte's bottle can flow into the soil column by connecting the Mariotte's bottle with the water inlet on the top cover of the soil column with a tetrafluoroethylene tube and opening the valve of the water inlet of the soil column. The water outlet was reserved at the bottom plate of the soil column, and the rate of water flow during the test can be calculated by the monitored water outflow.

3.3 Testing procedures

According to the *Standard for Geotechnical Testing Method* (GB/T50123–2019)[34] and the suggestions of Li et al.[32], the testing procedures of the combined determination method are described as follows:

(1) The soil sample was dried, crushed and then sieved through a 2 mm sieve. The dry soil was weighted to the desired mass and placed in the natural environment for 2 d. The soil column was compacted in 20 layers according to the set dry density until it reaches the designed dry density, and each layer was compacted to a thickness of 2 cm. When filling the next layer, the surface of the previous layer should be scratched to avoid the stratification of the soil column. During the filling process, the steel needle should be embedded at the sensor position in advance to facilitate the installation of the sensor.

(2) After the sample was filled, a perforated plate was placed on the upper surface of the soil column, and the quartz sand with a diameter of about 5 mm was placed on the perforated plate as a buffer layer to prevent the damage to the soil column sample. Then the moisture sensor was installed in the reserved position and sealed.

(3) The soil column sample was connected to the water supply device. In the WFAM test, the water head of 0 kPa was used for vertical infiltration. When the wetting front approaches the moisture sensor, the suction sensor was installed in the reserved hole (If the suction sensor was installed too early, the matric suction of soil exceeded the air inlet value of the ceramic head of the suction sensor, which would cause the suction sensor to fail. For the suction greater than the measurement range of the suction sensor, the pre-measured SWCC was used to obtain them). After the wetting front broke through the soil column for a period of time, IPM was used to conduct the test. In order to reduce the test duration, the water level was raised to 5 kPa. The test could be ended when the input and output flow reached a stable level.

(4) When disassembling the testing apparatus, the water content of the desiccated soil sample was measured by stratified sampling. The water content of the soil sample measured by the drying method was compared with the final reading of the moisture sensor, and the difference between them should be less than 1%. If the difference was greater than 1%, it should be checked whether the sensor was in close contact with the soil sample and the sensor should be recalibrated.

4 Test results and analysis

4.1 Data processing

The data processing procedures of the combined determination method are described as follows (taking the dry density of $\rho_d = 1.58$ g/cm^3 as an example, as shown in Fig. 4, in which θ_d is the characteristic water content):

(1) When the wetting front passes through the entire soil column, it is denoted as t_{out}. When $t < t_{out}$, the infiltration process does not conform to the linear assumption of IPM (see Section 5 for details). In this case, WFAM should be adopted to process the measured data:

① Draw the time–history curves of water content based on the measured data (see Fig. 4(a)).

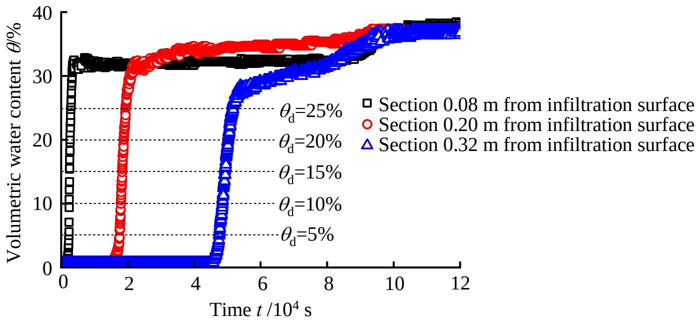

(a) Time–history curves of water content

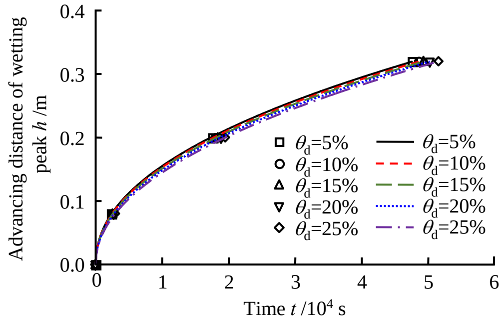

(b) Curves of wetting front advancing distance

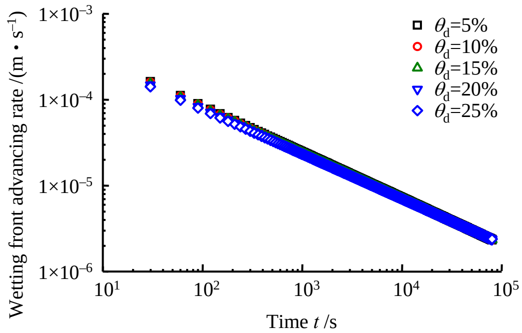

(c) Curves of wetting front advancing rate

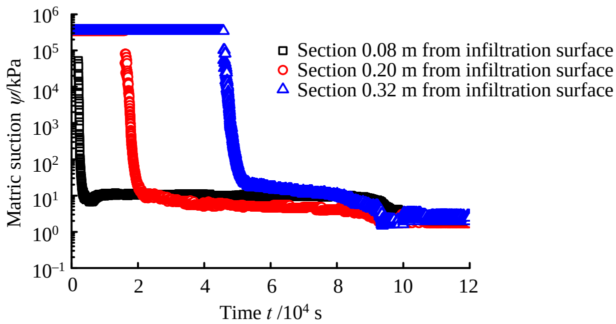

(d) Time–history curves of suction

Fig. 4 Data processing process of combined determination method

② Determine the curve of wetting front advancing distance $h(t)$. Different from the traditional observation method by the naked eyes, the digital wetting front method[32] was adopted in this study, i.e. the arrival of the wetting front at the monitoring section is characterized by the moisture sensor reading reaching the characteristic water content, θ_d, and then the time of the wetting front arriving at the monitoring section is recorded. Figure 4(a) shows the selection of θ_d. When the water content of the monitoring section increases to θ_d, it is considered that the wetting front advances to this position, and thus $h(t)$ can be obtained (see Fig. 4(b)).

③ Take the derivative of $h(t)$ to obtain the curve of wetting front advancing rate, $v(t)$ (see Fig. 4 (c)).

④ Based on the measured $\theta(t)$, the time–history curves of suction $\psi(t)$ (see Fig. 4 (d)) can be obtained according to the pre-measured SWCC (see Fig. 2 and Table 2) and the measured data of the suction sensor.

⑤ By substituting the measured $\theta(t)$, the converted $\psi(t)$ and the calculated $v(t)$ into Eq. (1), the hydraulic conductivity in the suction range of WFAM can be obtained.

(2) When $t \geqslant t_{out}$, WFAM is no longer applicable. At this point, IPM should be used to process the measured data. By substituting $\theta(t)$ and $\psi(t)$ measured at this stage into Eq. (2), the hydraulic conductivity in the suction range of IPM can be obtained.

4.2 Cumulative infiltration mass and water inflow and outflow rates

Figure 5 shows the cumulative infiltration mass and water inflow and outflow rates of three soil columns with various dry densities at different times. The test group with a dry density of 1.58 g/cm^3 was selected as an example to analyze the water infiltration process in the test. It can be seen from Fig. 5(a) that before the water level was raised, the growth rate ($\mathrm{d}m_w$ / $\mathrm{d}t$) of the cumulative infiltration mass of water m_w gradually decreased with time. In order to accelerate the infiltration rate and reduce the test duration, the water level was raised to 5 kPa to increase the water pressure. Due to the increase of water pressure, $\mathrm{d}m_w / \mathrm{d}t$ increased significantly, then gradually decreased and finally approached a constant, indicating that the seepage of soil column had reached a stable state. It can be seen from Fig. 5(a) that at the time of about 6.5×10^5 s (about 7.5 d), the water inflow and outflow rates finally tended to be identical, which also indicates that the seepage of soil column had reached a stable state at this time. The test results show that in this case, it only took about one week to complete the measurement of a set of hydraulic conductivities using the combined determination method. Compared to the traditional determination methods (steady state method and IPM), which take several months to measure the hydraulic conductivity, the combined determination method greatly reduces the test duration.

4.3 Variation of water content

Figures 4(a) and 6 show the time–history curves of water content, $\theta(t)$, of soil columns at sections 0.08, 0.20 and 0.32 m, respectively, from the infiltration surface under three dry densities. According to $\theta(t)$, the wetting process can be roughly divided into three stages: (1) the constant stage, i.e. when the wetting front does not reach the monitoring section, the soil water content is maintained at the initial water content; (2) the rapid increase stage, i.e. when the wetting front reaches the monitoring section, the soil suction drops rapidly, resulting in a large hydraulic gradient, and the water quickly enters the pores of dry soil; and (3) the slow increase stage, i.e. the wetting front has passed the sensor, and the soil water content increases slowly and tends to be stable.

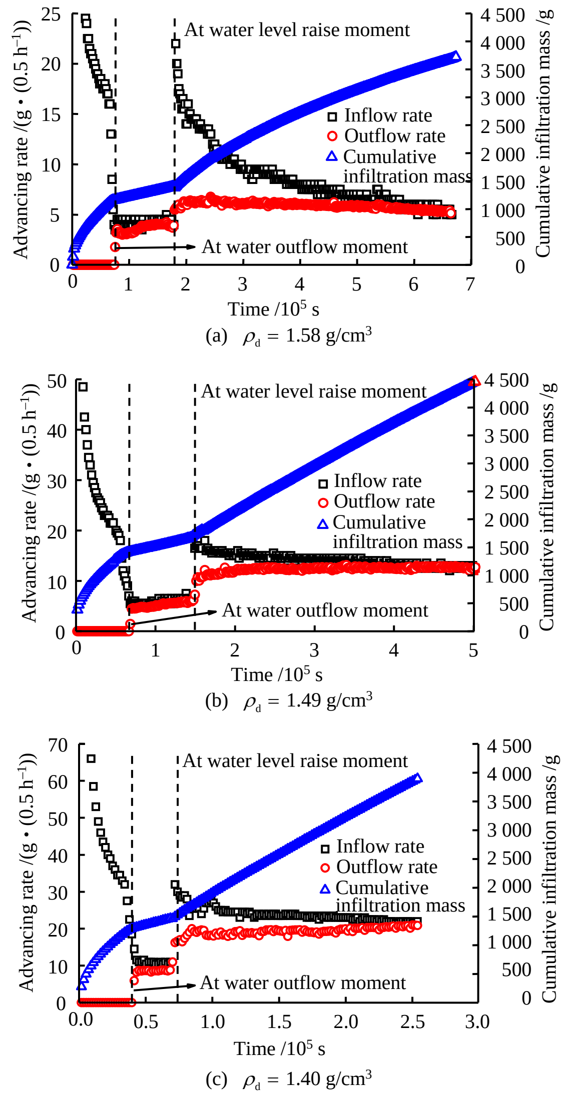

Fig. 5 Cumulative infiltration quality and inflow and outflow rates

It can be seen from the rapid increase stage of the three monitoring sections that the data points of the monitoring section at 0.08 m from the infiltration surface are relatively sparse, while the data points of the monitoring section at 0.32 m from the infiltration surface are denser. This indicates that the wetting front advancing rate v decreases with time.

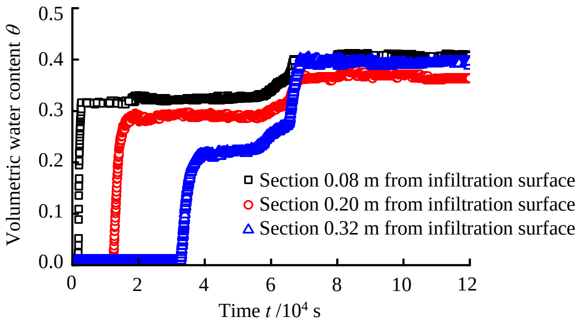

(a) ρ_d = 1.49 g/cm^3

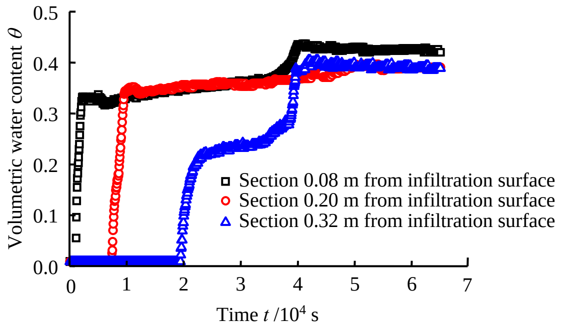

(b) ρ_d = 1.40 g/cm^3

Fig. 6 Time–history curves of water content at different monitoring sections

4.4 Wetting front advancing rate

In this study, the digital wetting front was used to judge the movement of the wetting front, and the characteristic water content θ_d selected at the rapid increase stage was adopted to represent the location of the wetting front. The method for selecting θ_d is illustrated in Fig. 4(a), and the water contents of 5%, 10%, 15%, 20% and 25% were selected as θ_d values. When the water content of the monitoring section increased to θ_d, it is considered that the wetting front advanced to this position, and the time is recorded as t_i. The advancing distance of wetting front h_i and time t_i under a certain θ_d are plotted in Fig. 4(b). By fitting the test curve in Fig. 4(b) with the power function and then differentiating the fitting curve, the variation of v with time can be obtained, as shown in Fig. 4(c).

It can be seen from Fig. 4(b) that under different θ_d values, the curves of wetting front advancing distance, $h(t)$, deviate slightly. With the increase of θ_d, $h(t)$ will shift rightwards on the axis of time, and this deviation becomes more apparently with the increase of the difference between the water content at this time and the initial water content. However, it can be seen from Fig. 4(c) that the v obtained under different θ_d values almost coincides, indicating that the selection of θ_d has little effect on v. For the same soil column, it can be seen from Eq. (1) that the selection of θ_d has little effect on the hydraulic conductivity. Therefore, it is reliable to use the digital wetting front to record the advancing position of the wetting front and then calculate the SHCF.

Figure 7 shows the curves of advancing distance and advancing rate of the wetting front under different dry densities. It can be found that for the soil with the same dry density, v gradually slows down as the infiltration proceeds. This is because with the increase of soil water content, the matric suction decreases, which leads to the decrease of hydraulic gradient. For soils with different dry densities, the greater the dry density is, the larger the v is. This is because the soil with higher dry density has smaller internal pores, which hinders the advance of the wetting front. In the follow-up study, Eq. (1) will be used to calculate the SHCF of soils with different dry densities according to the curves of wetting front advancing rate in Fig. 7(b).

4.5 Hydraulic conductivity function

Figure 8 shows the hydraulic conductivity of Qinghai silty clay in the full suction range under various dry densities measured by the combined determination method. It can be seen that WFAM and IPM can accurately measure the hydraulic conductivity in different suction ranges, and the measured values of the hydraulic conductivity in the overlapping range of suction are basically coincident. This indicates that the values of hydraulic conductivity measured by the two methods are reliable and the combination of these two methods can be used to determine the hydraulic conductivity in the full suction range. In addition, according to Section 4.1, it only takes about a week for the combined determination method to complete the measurement of a set of hydraulic conductivities. Therefore, this combined determination method can quickly determine the hydraulic conductivity in the full suction range.

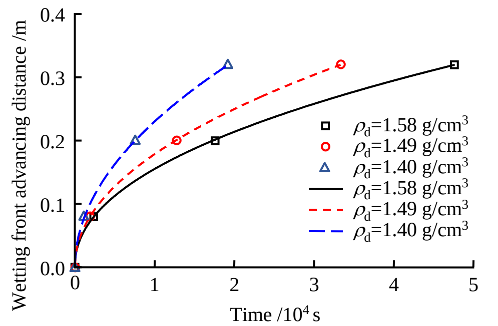

(a) Wetting front advancing distance under different dry densities

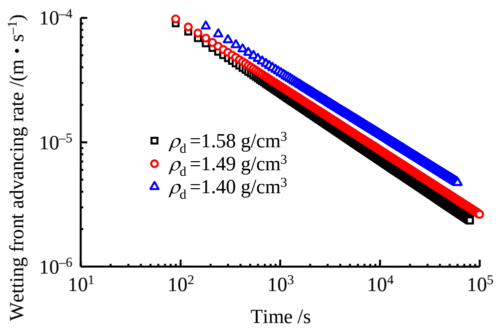

(b) Wetting front advancing rate under different dry densities

Fig. 7 Advancing distance and rate of wetting front under different dry densities

In this study, the Gardner model[38] was employed to fit the measured data. The Gardner model is expressed as

$$k(\psi)=\frac{k_s}{1+a\psi^n} \tag{3}$$

where k_s is the saturated hydraulic conductivity.

The Gardner model was used to fit the hydraulic conductivity of three soils with different dry densities, and the results are shown in Fig. 8. The coefficients of determination, R^2, in Fig. 8(a), (b) and (c) are 0.94, 0.97 and 0.94, respectively, indicating that the measurement results of the combined determination method can better reproduce the variation trend of the hydraulic conductivity in the full suction range.

For the case of a dry density of 1.58 g/cm^3 (Fig. 8(a)), when merely using the IPM data to fit the hydraulic conductivity, there is a large difference between the predicted values from the fitting curve in the high suction range and the measured values, i.e. IPM cannot reflect the variation of hydraulic conductivity in the high suction range; when merely using the WFAM data to fit the hydraulic conductivity, although it has a good fitting effect on the hydraulic conductivity in the high suction range, there are still some errors between the fitting results and the data measured by IPM in the low suction range, i.e. WFAM alone cannot reflect the variation of hydraulic conductivity in the full suction range; when using the combined data measured by WFAM and IPM, the measured data can better reflect the variation of hydraulic conductivity in the full suction range. The above analysis shows that the separate method can only reflect the hydraulic conductivity in the local suction range and cannot present the complete shape of the function of hydraulic conductivity. If the test results in the local suction range are used to fit SHCF in the full suction range, the inevitable errors will occur. Therefore, the combined determination method should be used to measure the hydraulic conductivity in the full suction range.

It can be seen from Fig. 8(d) that the test results of soil columns with different dry densities have the following characteristics. When $\psi \leqslant 60$ kPa, the influence of dry density on the hydraulic conductivity is obvious, and the hydraulic conductivity of soil increases with the decrease of dry density. When $\psi > 60$ kPa, the hydraulic conductivities of soil columns with different dry densities are almost the same, indicating that when the suction is high, the influence of dry density on the hydraulic conductivity can be ignored, which is consistent with the test results obtained in the literature[8, 39–41].

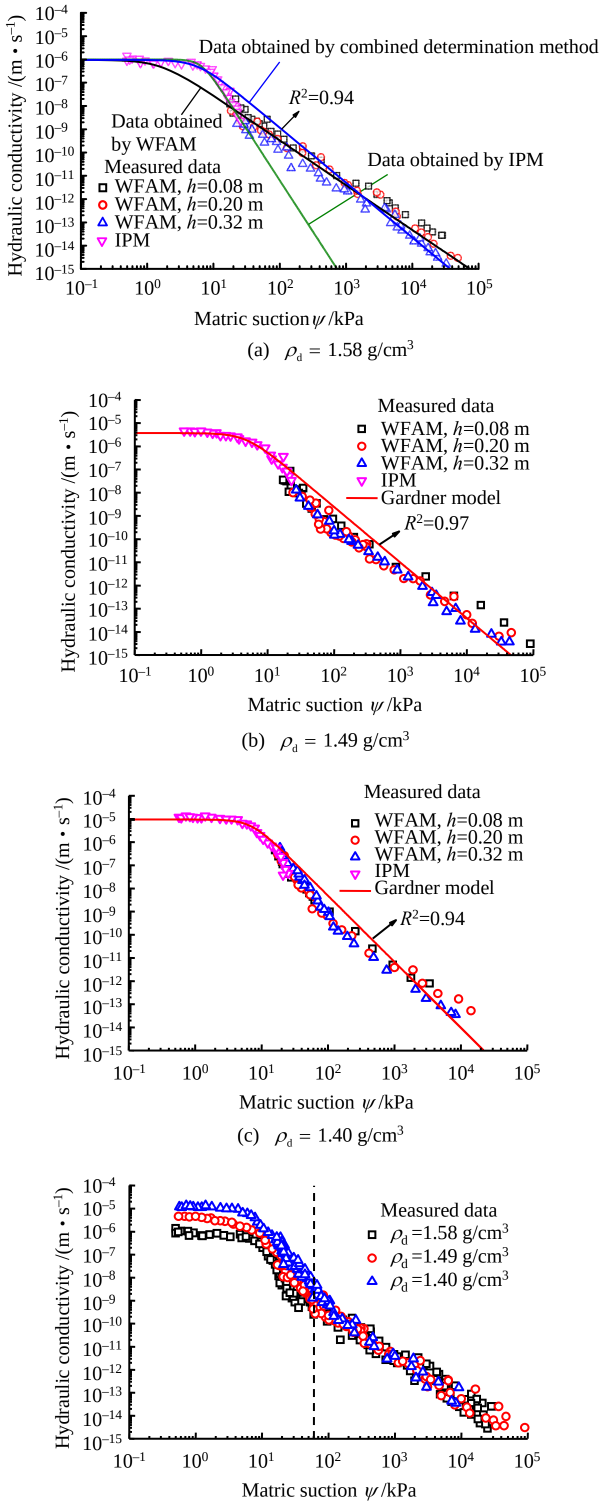

(a) ρ_d = 1.58 g/cm^3

(b) ρ_d = 1.49 g/cm^3

(c) ρ_d = 1.40 g/cm^3

(d) Comparison of measured results under different dry densities

Fig. 8 Hydraulic conductivity functions

5 Discussion

This study was carried out based on the combined determination method of WFAM and IPM. In order to achieve the rapid measurement of SHCF in the full suction range, it is unnecessary to use the soil with a higher initial water content and to maintain a larger infiltration rate in the test. The error sources and applicable ranges of WFAM and IPM in the combined determination method are discussed in detail below.

5.1 Error sources of WFAM and IPM

The section 0.20 m from the infiltration surface was selected as a representative, and the hydraulic gradients and flows calculated by IPM and WFAM were compared to analyze the error sources of WFAM and IPM in the combined determination method.

The hydraulic gradients obtained by IPM and WFAM at the section 0.20 m from the infiltration surface are plotted in Fig. 9, where i^- and i^+ are the hydraulic gradients calculated in the backward and forward directions at the section. As can be seen from Fig. 9, when $t < t_{out}$, there are large differences between i^-, i^+ and $(i^-i^+)^{0.5}$ calculated by IPM and the calculation duration is long, which is difficult to meet the linear assumption of IPM. i^-, i^+ and $(i^-i^+)^{0.5}$ calculated by WFAM are relatively close to each other. The hydraulic gradient is large sometimes, but it still satisfies the time-domain linear assumption of WFAM. When $t \geqslant t_{out}$, i^-, i^+ and $(i^-i^+)^{0.5}$ calculated by IPM are close to each other, which can be considered as conforming to the spatial linear assumption of IPM. Since the wetting front has disappeared at this stage, the hydraulic gradient calculated by WFAM loses its physical significance and WFAM is not applicable to this stage.

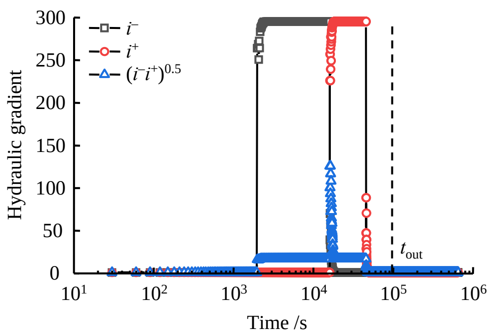

(a) Hydraulic gradient obtained by IPM

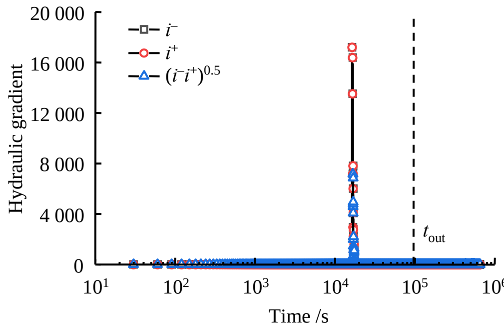

(b) Hydraulic gradient obtained by WFAM

Fig. 9 Hydraulic gradient at the section 0.20 m from infiltration surface

The section 0.20 m from the infiltration surface was selected as a representative, and the IPM and WFAM were used respectively to calculate the flow q. The measurement results are plotted in Fig. 10, where q calculated by IPM is denoted as q_{IPM}, and q calculated by WFAM is denoted as q_{WFAM}. It can be seen from Fig. 10 that when $t < t_{out}$, the flow calculated by the two methods is close, indicating that when $t < t_{out}$, the flow is close to the real flow, and the calculation error of hydraulic conductivity at this stage is caused by the hydraulic gradient of IPM. When $t \geqslant t_{out}$, it is found that $q_{IPM} > q_{WFAM}$. Since the wetting front has passed through the whole soil column at this time, the true v cannot be obtained, hence the q_{WFAM} obtained by calculation is incorrect. At this stage, the calculation error of hydraulic conductivity by WFAM is caused by its incorrect calculation of flow.

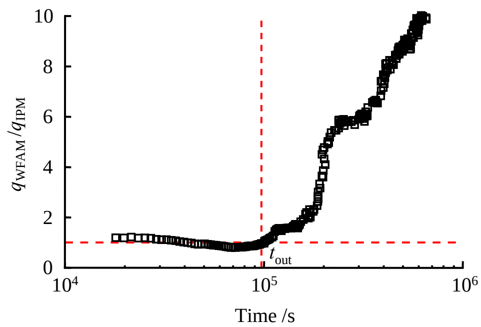

Fig. 10 Comparison of flow at the section 0.20 m from infiltration surface obtained by different methods

5.2 Application range of WFAM and IPM

Figure 11 shows the hydraulic conductivity calculated by IPM with three hydraulic gradients in the full suction range. Compared to the results obtained by WFAM, at the high suction stage ($\psi > 25$ kPa), the difference of the hydraulic conductivity calculated with i^- and i^+ is 4–7 orders of magnitude, which is obviously unacceptable. When $(i^-i^+)^{0.5}$ was adopted for calculation, the hydraulic conductivity obtained at $\psi < 1\ 251$ kPa roughly coincides with that obtained by WFAM, while the hydraulic conductivity obtained at $\psi > 1\ 251$ differs from that obtained by WFAM by 6 orders of magnitude. This indicates that it is unacceptable when $\psi > 1\ 251$ kP, thus IPM is not applicable to the determination of hydraulic conductivity in the high suction range. When the water comes out of the bottom ($t \geqslant t_{out}$), the whole soil column has been fully wetted. At this time, the wetting front has disappeared and the soil is at the low suction stage ($\psi \leqslant 25$ kPa), thus it is impossible to obtain the accurate value of v. As the hydraulic conductivity calculated by WFAM is incorrect, WFAM is not suitable for determination of the hydraulic conductivity at the low suction stage. The test results in Fig. 11 also confirm the analysis results presented in Figs. 9 and 10.

To sum up, in the combined determination method, WFAM is suitable for the case that the wetting front has not passed through the whole soil column yet ($t < t_{out}$), i.e. the high suction range ($\psi > 25$ kPa), while IPM is suitable for the case that the wetting front has passed through the whole soil column ($t \geqslant t_{out}$), i.e. the low suction range ($\psi \leqslant 25$ kPa).

DOI: 10.16285/j.rsm.2022.5004

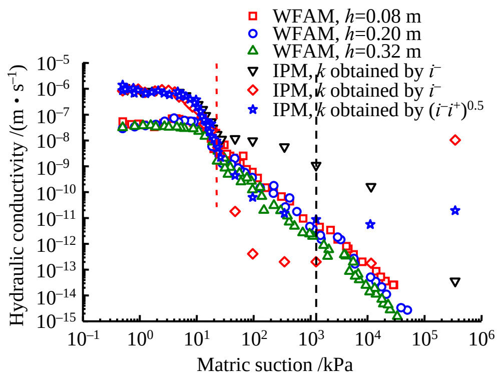

Fig. 11 Comparisons of WFAM and IPM in the full suction range

5.3 Type of soil applicable to combined determination method

The combined determination method can be applicable to the common sand, silt and clay in some unsaturated soil problems. However, special attention should be paid to the size effect when using this method in coarse-grained soils, and it is better to set a reasonable mold diameter according to the maximum particle size of the soil. When the particle size of the soil is too large, the probe of the moisture sensor may not be in close contact with the soil, and it is difficult to obtain an effective reading. For very dense clay, such as densely compacted Gaomiaozi bentonite, the instrument may be damaged due to the water absorption and swelling properties. In addition, the hydraulic conductivity of dense clay is relatively low, ranging from 10^{-13} to 10^{-15} m/s[20]. If the test is conducted with a water head of 0 kPa, the test duration may take several months, thus a higher infiltration water head should be used to reduce the test duration. For undisturbed clay, due to the difficulty of sample preparation and installation, it is necessary to specially design the sampler and reprocess the test device (such as two-half mold or three-half mold) for testing.

There are two common ways to control the dry density of soil samples. One is to prepare samples with the given initial dry density and initial water content. The other method is to prepare samples with the given initial water content and compaction work and then back-calculate the dry density after sample disassembly. For silty soil, when the initial water content is close to the optimum water content, the soil column can reach the maximum dry density, at which the soil has a higher water content. Therefore, it is difficult to obtain the hydraulic conductivity of the soil lower than this water content, which means that it is impossible to measure the hydraulic conductivity of soil in the full suction range. When the soil with initial water content close to 0 is used for testing, the soil cannot be compacted to the maximum dry density, thus it is necessary to design the dry density required by the test according to the physical conditions of the soil at the measured site. As for the Qinghai silty clay used in this study, the test results showed that when it approaches dry soil, the maximum degree of compaction it can achieve is 0.93, and the corresponding dry density is 1.63 g/cm^3. Therefore, the dry density $\rho_d <$ 1.63 g/cm^3 is selected in this study.

6 Conclusions

(1) WFAM and IPM can better measure the hydraulic conductivity in different suction ranges. In the overlapping suction range, the measurement results from the two methods are basically coincident, and the test duration is reduced from several months to about a week, which shows that the combined determination method can achieve rapid measuring of soil hydraulic conductivity in the full suction range. Therefore, the feasibility of using the combined determination method is proved and the SHCF measurement is expected to become a routine test in soil mechanics for unsaturated soils.

(2) In the combined determination method, before the wetting front passes through the whole soil column ($t < t_{out}$), due to the excessive infiltration rate, the hydraulic gradient of IPM at this stage produces a large error, which does not conform to the linear assumption of IPM. When the wetting front has passed through the whole soil column ($t \geqslant t_{out}$), it is difficult to obtain the accurate v at this stage, resulting in errors in the flow determined by WFAM at this stage.

(3) In the combined determination method, WFAM is applicable to the measurement of the hydraulic conductivity in the high suction range ($\psi > 25$ kPa) before the wetting front passes the whole soil column ($t < t_{out}$). IPM is applicable to the measurement of hydraulic conductivity in the low suction range ($\psi \leqslant 25$ kPa) after the wetting front has passed the whole soil column ($t \geqslant t_{out}$).

References

[1] MUALEM Y. Hydraulic conductivity of unsaturated porous media: generalized macroscopic approach[J]. Water Resources Research, 1978, 14(2): 325–334.

[2] FREDLUND D G, XING A, HUANG S. Predicting the permeability function for unsaturated soils using the soil-water characteristic curve[J]. Canadian Geotechnical Journal, 1994, 31(4): 533–546.

[3] LEONG E C, RAHARDJO H. Permeability functions for unsaturated soils[J]. Journal of Geotechnical and Geoenvironmental Engineering, 1997, 123: 1118–1126.

[4] ZHAI Q, RAHARDJO H. Estimation of permeability function from the soil–water characteristic curve[J]. Engineering Geology, 2015, 199: 148–156.

[5] ROMERO E, GENS A, LLORET A. Water permeability, water retention and microstructure of unsaturated compacted Boom clay[J]. Engineering Geology, 1999, 54(1–2): 117–127.

[6] LI J H, ZHANG L M, LI X. Soil-water characteristic curve and permeability function for unsaturated cracked soil[J]. Canadian Geotechnical Journal, 2011, 48(7):

1010–1031.

[7] HU R, CHEN Y F, LIU H H, et al. A water retention curve and unsaturated hydraulic conductivity model for deformable soils: consideration of the change in pore-size distribution[J]. Géotechnique, 2013, 63(16): 1389–1405.

[8] LI Yan, LI Tong-lu, HOU Xiao-kun, et al. Prediction of unsaturated permeability curve of compaction loess with pore-size distribution curve and its application scope[J]. Rock and Soil Mechanics, 2021, 42(9): 2395-2404.

[9] WANG Hai-man, NI Wan-kui. Prediction model of saturated/unsaturated permeability coefficient of compacted loess with different dry density[J]. Rock and Soil Mechanics, 2022, 43(3): 729–736.

[10] LI X, LI J H, ZHANG L M. Predicting bimodal soil–water characteristic curves and permeability functions using physically based parameters[J]. Computers and Geotechnics, 2014, 57: 85–96.

[11] ZHANG Zhao, CHENG Jing-xuan, LIU Feng-yin, et al. Physical approach to predict unsaturated permeability function based on soil particle size distribution[J]. Rock and Soil Mechanics, 2019, 40(2): 549–560.

[12] MEERDINK J S, BENSON C H, KHIRE M. Unsaturated hydraulic conductivity of two compacted barrier soils[J]. Journal of Geotechnical Engineering, 1996, 122(7): 565–576.

[13] GALLAGE C, KODIKARA J, UCHIMURA T. Laboratory measurement of hydraulic conductivity functions of two unsaturated sandy soils during drying and wetting processes[J]. Soils and Foundations, 2013, 53(3): 417–430.

[14] HUANG S, FREDLUND D G, BARBOUR S L. Measurement of the coefficient of permeability for a deformable unsaturated soil using a triaxial permea-meter[J]. Canadian Geotechnical Journal, 1998, 35(3): 426–432.

[15] SAMINGAN A S, LEONG E, RAHARDJO H. A flexible wall permeameter for measurements of water and air coefficients of permeability of residual soils[J]. Canadian Geotechnical Journal, 2003, 40(3): 559–574.

[16] RICHARDS A L, WEEKS L. Capillary conductivity values from moisture yield and tension measurements on soil columns[J]. Soil Science Society of America Journal, 1953, 17(3): 206–209.

[17] CUI Y J, TANG A M, LOISEAU C, et al. Determining the unsaturated hydraulic conductivity of a compacted sand-bentonite mixture under constant-volume and free-swell conditions[J]. Physics and Chemistry of the Earth, Parts A/B/C, 2008, 33: S462–S471.

[18] WANG Q, CUI Y, TANG A M, et al. Hydraulic conductivity and microstructure changes of compacted bentonitesand mixture during hydration[J]. Engineering Geology, 2013, 164: 67–76.

[19] YE W M, CUI Y J, QIAN L X, et al. An experimental study of the water transfer through confined compacted GMZ bentonite[J]. Engineering Geology, 2009, 108(3): 169–176.

[20] YE Wei-min, QIAN Li-xin, CHEN Bao, et al. Laboratory test on unsaturated hydraulic conductivity of densely compacted Gaomiaozi bentonite under confined conditions[J]. Chinese Journal of Geotechnical Engineering, 2009, 31(1): 105–108.

[21] NIU W, YE W, SONG X. Unsaturated permeability of Gaomiaozi bentonite under partially free-swelling conditions[J]. Acta Geotechnica, 2020, 15(5): 1095–1124.

[22] LIU Z, CUI Y, YE W, et al. Investigation of the hydro-mechanical behaviour of GMZ bentonite pellet mixtures[J]. Acta Geotechnica, 2020, 15(10): 2865–2875.

[23] HU Hai-jun, LI Chang-hua, CUI Yu-jun, et al. Research on the determination of permeability coefficient of unsaturated remolded loess under wetting condition[J]. Journal of Hydraulic Engineering, 2018, 49(10): 1216–1226.

[24] HU H J, CUI Y J, LI C H, et al. Improvement of three common methods for determining hydraulic conductivity curve of unsaturated soil upon wetting[J]. Journal of Hydrology, 2021, 594: 125947.

[25] LI X, ZHANG L M, FREDLUND D G. Wetting front advancing column test for measuring unsaturated hydraulic conductivity[J]. Canadian Geotechnical Journal, 2009, 46(12): 1431–1445.

[26] MIAO Qiang-qiang, CHEN Zheng-han, TIAN Qing-yan, et al. Experimental study of capillary rise of unsaturated clayey sand[J]. Rock and Soil Mechanics, 2011, 32(Suppl.1): 327–333.

[27] LI Xu, FAN Yi-kai, HUANG Xin. Applicability of the wetting front advancing method for measuring hydraulic conductivities of unsaturated soil[J]. Rock and Soil Mechanics, 2014, 35(5): 1489–1494.

[28] LIU Li, WU Yang, CHEN Li-hong, et al. Accuracy analysis of wetting front advancing method based on numerical simulation[J]. Rock and Soil Mechanics, 2019, 40(Suppl.1): 341–349.

[29] QIN Xiao-hua, LIU Dong-sheng, SONG Qiang-hui, et al. Experimental study on one-dimensional vertical infiltration in soil column under rainfall and the derivation of permeability coefficient[J]. Chinese Journal of Rock Mechanics and Engineering, 2017, 36(2): 475–484.

[30] LIU Q, XI P, MIAO J, et al. Applicability of wetting front advancing method in the sand to silty clay soils[J]. Soils and Foundations, 2020, 60(5): 1215–1225.

[31] CAI Guo-qing, LIU Qian-qian, YANG Yu, et al. Seepage experiments of sandy loess soil column with different stress states based on wetting front advancing method[J]. Journal of Hydraulic Engineering, 2021, 52(3): 291–299.

[32] LI X, ZHANG Z, ZHANG L, et al. Combining two methods for the measurement of hydraulic conductivity over a wide suction range[J]. Computers and Geotechnics, 2021, 135: 104178.

[33] DANIEL D E. Measurement of hydraulic conductivity of unsaturated soils with thermocouple psychrometers[J]. Soil Science Society of America Journal, 1982, 46(6): 1125–1129.

[34] Ministry of Water Resources of the People's Republic of China. GB/T50123－2019 Standard for geotechnical testing method[S]. Beijing: China Planning Press, 2019.

[35] LI Xu, LIU A-qiang, LIU Li et al. A rapid method for determining the soil-water characteristic curves in the full suction range[J]. Rock and Soil Mechanics, 2022, 43(2): 299–306.

[36] VAN GENUCHTEN M T. A closed-form equation for predicting the hydraulic conductivity of unsaturated soils[J]. Soil Science Society of America Journal, 1980, 44(5): 892–898.

[37] MCCARTHY E L. Mariotte's bottle[J]. Science, 1934, 80(2065): 100.

[38] GARDNER W R. Some steady state solutions of the unsaturated moisture flow equation with application to evaporation from a water table[J]. Soil Science, 1958, 85(4): 228–232.

[39] TAO Gao-liang, WU Xiao-kang, GAN Shi-chao, et al. Experimental study and model prediction of permeability coefficient of unsaturated clay with different initial void ratios[J]. Rock and Soil Mechanics, 2019, 40(5): 1761–1770.

[40] LI Hua, LI Tong-lu, ZHANG Ya-guo, et al. Relationship between unsaturated permeability curve and pore-size distribution of compacted loess with different dry density[J]. Journal of Hydraulic Engineering, 2020, 51(8): 979–986.

[41] LIU Li, WU Yang, LI Xu, et al. Influence of compaction on hydraulic properties of widely-graded soil[J]. Rock and Soil Mechanics, 2021, 42(9): 2545–2555.